The author(s) shown below used Federal funding provided by the U.S. Department of Justice to prepare the following resource:

Document Title:	**Expanding the Scope and Efficiency of 3D Surface Topography Analysis in Firearm Forensics**
Author(s):	**Ryan Lilien**
Document Number:	**304618**
Date Received:	**April 2022**
Award Number:	**2019-DU-BX-0012**

Final Research Report - Cover Page

Federal Agency and Organization Element: Department of Justice, National Institute of Justice

Federal Grant or Other Identifying Number: 2019-DU-BX-0012

Project Title: Expanding the Scope and Efficiency of 3D Surface Topography Analysis in Firearm Forensics

PD/PI Name, Title, Contact Info: Ryan Lilien, Chief Scientific Officer, Cadre Research Labs; 500 Davis Street, Suite 500; Evanston, IL 60201

Name of Submitting Official: Ryan Lilien

Submission Date: Sept 29, 2021

Recipient Organization: Cadre Research Labs, LLC (small business)

Recipient Identifying Number (if any): N/A

Project/Grant Period: Start: 1/1/2020, End: 6/30/2021

Signature of Submitting Official:

1 Project Purpose and Background

The comparison of cartridge cases and bullets is based on the observation that microscopic firearm imperfections (such as those on a breech-face, barrel, or firing-pin) can be transferred to ammunition during firing. The ability to certify two items as similar is therefore a function of both the ability to capture and visualize a high-resolution measurement of each specimen and the ability to identify and match relevant structural features between the two. Courtroom challenges and recent reports have called for additional research into underlying error rates and performance measures for these comparative methods.

The aims of this proposal develop and evaluate new technology in support of toolmark examination. The work represents an important milestone for our previously funded NIJ projects. Over the past few years the NIJ has helped support development of our technology for 3D topographic imaging and analysis of cartridge cases. The aims of this proposal include extending our methodology to bullets (Aim 1) and evaluating the use of a portable scanner within the crime lab (Aim 2). We are proud that our technology is beginning to have real impact in the crime lab. In 2017, the FBI Firearm and Toolmark Unit successfully completed a validation study of our 3D imaging hardware and visualization software and is now live using the system in casework. In 2019, the Canadian RCMP achieved the same milestone. Several city and state level labs are at various stages of validation. To improve the rate of adoption, it is critical to add bullet scanning to the system's capabilities (Aim 1). In addition, the availability of a portable scanning system (Aim 2) will allow more labs to incorporate 3D VCM and will allow labs to identify novel as-yet unknown uses for 3D scanning technology. In Aim 1 we will develop tools for high-resolution scanning and analysis of bullets. In Aim 2 we will evaluate the use of a portable 3D scanning system within the crime lab. Both aims represent important next steps for our emerging technology.

1.1 Transition to 3D Measurements

Several shortcomings of traditional toolmark examination can make comparison difficult [1]. For example, lighting effects (*i.e.,* shadows) can adversely affect 2D image interpretation. Automated comparison algorithms that rely on 2D images are therefore dependent on consistent orientation and lighting position. Even when the imaging setup is consistent, many surface features are simply not resolvable with 2D technologies. In addition, traditional comparison light-microscopy suffers from a physical access

requirement. That is, examination requires physical access to the specimens. This may necessitate potentially burdensome chain-of-custody documentation and introduces the opportunity for evidence to be damaged or lost.

To address these issues, new technologies, capable of measuring 3D surfaces, are now being evaluated [2, 18, 20]. Some of these technologies, including our GelSight-based scanner, measure accurate 3D surface topographies in standard units resulting in a detailed heightmap of the specimen surface. This true measurement data can be exchanged between systems using a common file format. In collaboration with NIST, Cadre leads the OpenFMC (Open Forensic Metrology Consortium) working group which seeks to promote this type of data exchange. Comparison algorithms are being developed to analyze 3D surface topographies [6, 11, 13, 14, 16, 21, 22] and may soon provide statistical interpretations to their match scores (*e.g.*, a false match rate).

The topographic data acquired from 3D scanners can be used in the emerging application of Virtual Comparison Microscopy (VCM). Initially introduced by Senin *et al.* [12] in 2006, VCM describes the visual examination of a 3D microscopic representation of an object. In VCM, the examiner views and manipulates the object's measured 3D representation using a computer without physical access to the specimen. The lack of a physical access requirement allows several advantages across the areas of: Access & Archiving Evidence, Training, Proficiency/Error-Rate Studies, Verifications, and Algorithmic Comparison. VCM systems can also include a number of features or functions that are difficult if not impossible to perform on a traditional light microscope. For example, the ability to recall exact specimen and light positions from session to session and the ability to simultaneously display more than two items. For these reasons, the past few years have seen significant interest and movement towards 3D imaging.

1.2 Development of a 3D VCM System

Since we began development of a GelSight-based 3D VCM system, grants from NIJ have played an important role. Over the past few years we've developed technology capable of measuring the 3D surface topographies of cartridge cases at micron-scale resolution (Fig. 1). Our approach utilizes advanced three-dimensional imaging algorithms (*e.g.*, shape from shading and photometric stereo) and the GelSight sensor [7, 8]. Our sensor is a block of optically clear elastomer with a thin layer of elastic paint on one side (Fig. 1). When an object is pressed into the elastomer, the layer of paint conforms to the shape of the surface. The paint removes the influence of the optical properties of the surface on shape measurement. In contrast to confocal and focus-variation microscopy, this important feature of our system removes

several negative influences of surface reflectivity on the measured topography. For example, the gel-based imaging approach allows our system to capture fine striations which may appear washed out when measured via other technologies. The ability to measure fine striations is important for the bullet imaging completed in Aim 1.

Over the past several years, we developed our system from a prototype manual rig, into a single cartridge case loading fixture, and then into our current tray-based batch scanning system. Our current tray holds up to fifteen cartridge cases on a movable stage. Under software control, the system positions each holder under the gel, raises the holder into the gel, focuses the camera, sequentially illuminates a set of lights (Fig. 1), and captures a sequence of images. The collected images are used to compute the surface normals using nonlinear least-squares optimization and the three-dimensional surface by integration. The scalar value recorded at each pixel is the surface height of the object at the corresponding location. The batch scanner reduces scan acquisition time while improving scan consistency. Measurements can be made traceable by calibrating with a traceable reference standard. The interested reader is referred to [3, 7, 8, 21] for additional detail.

2   Project Design

The one year project included two aims which continued the R&D of our novel technology to advance 3D Virtual Comparison Microscopy. The proposed aims advance the discipline of firearm and toolmark examination by developing and improving tools for 3D virtual comparison microscopy of cartridge cases and bullets. In Aim 1 we extended our 3D VCM technology to the scanning and comparison of bullets. In the second aim we expanded the accessibility and use of 3D virtual comparison microscopy via evaluation of our portable scanning system.

In completion of Aim 1 we developed an automated bullet scanning process and then evaluated that process on a small set of test fires. The bullet scanning process uses a batch scanning tray that fits into our current scanner platform. It therefore requires no changes to the core scanning subsystem (*i.e.*, camera, lens, or gel-based sensor). Our process was tested / demonstrated with a small set of test fires collected for this study. In Aim 2 we completed a scanning study with our portable scanner. A core set of test fired cartridge cases was scanned by four individuals using two portable systems and our desktop system. Scans were compared to demonstrate the scan quality and consistency of the portable unit. Both aims were successfully completed during the project period.

NOTE: Please note that we encountered two significant events which affected our timeline and our ability

to complete the initial proposed research. The covid19 pandemic greatly affected the type of work that could be safely conducted. The second event was the NIJ transition to JustGrants and ASAP for grant management and reimbursement. Getting our organization and grant into the new system took a long time during which our activities were put on hold. Technical support bounced us between several agencies. A report from the Inspector General confirms that we were not alone in experiencing these problems. They report that over 1000 organizations were still not transitioned as of March 2021. Fortunately we were only delayed by about six months. We were given a grant extension to June 2021 to allow for the covid and JustGrants/ASAP system delays.

3   Materials and Methods

In this section we describe the general approach for each aim. We describe the tools developed and datasets used. In the Results and Analysis section we describe and interpret the obtained results.

3.1   Bullet Scanning and Analysis (Aim 1)

Bullet analysis typically relies on the examination of striated toolmarks transferred onto one of several Land Engraved Areas (LEAs). The important and individualizing toolmark information is contained within the striation pattern of these LEAs. Three-dimensional bullet analysis therefore involves scanning LEAs, extracting striation profiles, and then either visually or algorithmically comparing these profiles. In Aim 1 we proposed to extend our 3D scanning platform to scan and compare bullet LEAs. Prior to the project we completed a proof-of-concept experiment with a fixed curved plastic base capable of holding a single caliber of bullet in a fixed position. In Aim 1, we extended this initial design into a more general purpose and automated mount fixture and then integrated the use of this fixture into our scan acquisition software. We proposed to scan a set of known match (KM) paired test fires to demonstrate that the holder functioned on a range of calibers. We noted that bullets are often damaged when they impact hard surfaces such as walls. We wanted to explore as proof-of-concept how we could scan bullets that were partly or significantly damaged. Finally, we wanted to explore the analysis of these extracted profiles using comparison algorithms. We note that individual marks, potentially useful for source identification, can be found in Groove Engraved Areas (GEAs) and along the entire bullet bearing surface. While this project focused on the analysis of LEAs many of our scans did pickup additional marks such as GEAs and slippage marks. Our firearms examiner collaborators were excited to see these marks on the scans

and are interested to see how they could be used in a future project.

3.1.1 Bullet Tray

One piece of feedback we frequently receive on our current cartridge case scanning setup is that the system is extremely easy to use. In contrast to general-purpose 3D microscopes which require the correct adjustment of dozens of settings, dials, and parameters, our system is optimized for the 3D scanning of firearm and toolmark specimens. Over the past several years we put great effort into making our scanning tray and software easy to use. We took the same approach in this project when designing the bullet holder, bullet tray, and scan acquisition software.

In this project we designed a bullet scanning tray (Fig. 2) with the same outer dimensions as our current cartridge case tray. The new tray therefore fits into the mounting brackets of our desktop's motorized stage and allows batch scanning. Rather than accept fifteen-cartridge cases, the bullet tray accommodates two bullets and three microscale references. Each bullet holder can move up and down within the tray and can be removed from the tray entirely. In each bullet holder (Fig. 2A) the bullet is supported by two rubber rollers (Fig. 2D) and is held in place with a spring loaded mount rod (Fig. 2B). The rod has a rubber tip (Fig. 2C) that captures the bullet nose. The base of the bullet sits on a plastic spring loaded peg (Fig. 2F). The spring loaded rod (Fig. 2B) allows the operator to rotate the mounted bullet. An important detail of the holder is that the spacing of the rubber rollers (Fig. 2D) can be adjusted by a set screw on the bottom of the holder. Moving the rubber rollers adjusts the height of the bullet. Bullets with smaller diameter require that the rollers be closer together. Bullets with larger diameters require the rollers to be further apart. The range of roller positions can accommodate all commonly encountered calibers.

Microscale references required by the system such as the Ball Grid Array and sinusoid reference can be mounted in the first column of the tray (Fig. 2E). The slots in the first column accept the same size microscale reference holders as our cartridge case tray which allows the same references to be used both with the cartridge case tray and the bullet tray.

Bullets mount in only one direction and scanning proceeds in a single direction so that the order of LEA scanning is consistent. The bullet holder (the tray insert, not the tray itself) can be removed from the tray and used with the portable scanner. The portable scanner lacks the motorized automation of the desktop scanner and so rotation between LEAs is accomplished by the knob attached to the spring loaded mount rod.

3.1.2 Bullet Rolling

In Aim 1 we developed a technique for automatic rolling of a bullet such that the entire circumference of the bearing surface can be scanned without manual user intervention. Photos and an illustration of the rolling process appear in Figure 3. During scanning a motorized lift platform guided by a force sensor raises the bullet into the gel, the system is focused, and a sequence of directional light images are collected allowing measurement of that frame's 3D surface topography. After the measurement is taken a bullet roll is initiated by the software to move the bullet to the next position. From the starting position (Fig. 3A) the motorized platform slides the bullet holder slightly to the left (arrow) while the holder is still raised and the bullet is still making contact with the gel. Both the bullet and red rollers spin as the gel grabs the contact surface (Fig. 3 B and C). The linear shift results in a rotation of the mounted bullet. The holder is then lowered and shifted back to recenter the now rotated bullet under the gel (Fig. 3D). The motorized lift platform raises the rotated bullet into the gel (Fig. 3E). Large rotations may require more than one cycle through A-E.

3.1.3 Scan Acquisition Software and the Scanning Process

We added new functionality to our TopMatch software to support bullet scanning. A workflow was added to interface with the bullet tray. Scanning involves cleaning the specimen and mounting the bullet nose behind the rubber cap of the mount rod (Fig. 2B) of the bullet holder (Fig. 2A) in the bullet tray. If necessary, the spacing of the rubber rollers is adjusted so that the center of the bullet is co-linear with the axis of the mount rod. Finally the rod is rotated to rotate the bullet such that the first LEA is positioned on the top of the bullet (facing up). It was our aim to make scan acquisition extremely simple. After specifying the bullet item numbers in the software the tray is inserted into the scanner and the user clicks to start the scan. The entire scanning process is automated except for the first focus adjustment. That is, after the system raises the bullet into the gel and the system performs an initial focus, the user is able to make a focus adjustment. After accepting the focus, the automatic rotation mechanism (Section 3.1.2) allows automatic scanning of the entire bullet circumference without manual intervention. That is, once the user sets the initial focus in the initial frame the system handles the rest.

3.1.4 Damaged Bullets

It is not uncommon for evidence bullets to be recovered in a damaged or mangled state. These deformed bullets are difficult for any scanning system to measure as metal deformation may physically interfere

with the view of the land engraved area. In addition to water tank shot 'pristine' bullets, we collected several types of damaged bullets to demonstrate initial feasibility of scanning each type of damage. Three conditions of damage are considered:

- **Ricochet Bullets**: (Figure 4 B) These bullets were ricocheted off a hard surface and their cross section is no longer circular. They may also have overall shape deformation. The deformed shape needs to be considered during scanning.

- **Mushroomed Bullets**: (Figure 4 C) These are hollowpoint bullets with petals that have folded back on the bullet itself. The petals often interfere with the optical path to the LEAs.

- **Bullet Fragments**: (Figure 4 D) A single bullet can break into several small fragments. There are many causes of bullet fragmentation. Fragmentation may occur when the bullet hits soft tissue or a hard surface. One common way for fragments to form is for a petal of a hollow-point bullet to fold back and detach from the jacket or core. This is the method we used to generate bullet fragments.

Images of test fired bullets that we collected corresponding to these three conditions appear in Figure 4. We are able to load most ricochet bullets in the holder described in Section 3.1.1. For mushroomed and fragmented specimens we used plastic tools to bend and expose the bearing surface. For fragmented bullets we used a specimen holder with a flat foam surface. For larger fragments and mushroomed specimens we used mounting putty to position the specimen at a desired angle for scanning.

3.1.5   Bullet Comparison

Acquired scans can be analyzed via Virtual Comparison Microscopy where the examiner loads two specimens and compares the measured surfaces for similarities and differences. Acquired scans can also be compared via a comparison algorithm that measures and reports a quantitative measure of similarity. The first step in algorithmic comparison of striated toolmarks is for the operator to mask (*i.e.*, highlight) the region of interest. For bullets this is typically the LEAs described above. The second step in analysis is for the comparison algorithm to extract the linear striation profile from the masked region. Over the past several years we developed a robust method for extracting striation profiles from measured surfaces. This method automatically removes the baseline and identifies both the shearing direction (by examination of the surface gradients) and the direction perpendicular to the shearing direction. It is along this perpendicular direction that the linear profile is extracted.

Once the linear striation profiles of two scans are extracted they can be compared using one or more methods. Supported by a separate grant we implemented a version of NIST's Congruent Matching

Profile Segments (CMPS) comparison algorithm [4, 15]. The CMPS method is designed to compare striated toolmarks such as those seen on land engraved areas. The unique information in a striated mark is contained in its linear profile and not in its overall surface [9, 10, 17]. CMPS is based on the identification and matching of small profile segments. The general idea of CMPS is to first split one striation profile into a series of small segments and then match each segment against the second striation profile. The number of segments for which a consistent offset results in sufficient profile similarity are counted. Similar profiles will have a large number of matched segments whereas dissimilar profiles will have a smaller count.

The ability to determine the number of CMPS segments between two profiles (*e.g.*, two LEAs) is only the first step of comparing two bullets. To obtain a score for the comparison of two bullets one must consider all possible phases (aka alignments) between the two bullets and combine the similarity scores of all corresponding LEAs from that alignment. For bullets with six LEAs, if LEA 1 in the first bullet corresponds to LEA 1 in the second bullet then the overall correspondence is 1:1, 2:2, 3:3, 4:4, 5:5, and 6:6 where each X:Y pair indicates that LEA X of the first bullet corresponds to LEA Y of the second bullet. We can add the CMPS scores for each of these six comparisons to get the bullet to bullet score. If however LEA 1 of the first bullet corresponds to LEA 2 of the second bullet then the overall correspondence is 1:2, 2:3, 3:4, 4:5, 5:6, and 6:1 and the total bullet to bullet score would consist of the sum of CMPS scores for these comparisons. Thus for two bullets with 6 LEAs one must consider a total of six different shifts for each bullet to bullet comparison. The score of the bullet to bullet comparison is the maximum value of these six possibilities. This CMPS-Sum score is used in the results section. Note that LEA ordering may be unknown for damaged bullets where the original structure of the bullet can not be inferred.

3.2   Firearm Test Sets (Aims 1 and 2)

Our collaborator Zak Carr selected twelve firearms for use in both aims. Bullets from ten of these firearms were used in Aim 1 (Bullet Scanning) and cartridge cases from all twelve of these firearms were used in Aim 2 (Portable Scanner Experiment). The selected firearms appear in Table 1. The firearms were selected to represent three calibers commonly encountered in casework (9mm Luger, .40 S&W, and 45 Auto). The cartridge cases from these firearms include a range of class. Figures 9 and 10 show one test fire from each of the twelve firearms. Some of the bullets are well marked and some are less well marked. Some have essentially no stria in their LEAs. Although not the focus of this project, many of

the firearms produce potentially useful Groove Engraved Areas (GEAs) and some have well visualized slippage marks.

Test fire collection proceeded as follows. The pristine FMJ (full metal jacket), pristine JHP (jacketed hollowpoint), and mushroomed JHP (jacketed hollowpoint) bullets were collected by firing into a water recovery tank. Pristine JHP bullets were fired with the nose cavity plugged with putty to prevent expansion. This was to provide an undamaged exemplar to be compared to other mushroomed/damaged bullets of the same brand. Mushroomed JHP bullets did not receive any treatment to prevent the expansion of the hollow point cavity. Ricochet bullets were fired by using a piece of bullet-resistant polycarbonate and a Kevlar bullet collection box. The polycarbonate was NIJ level IIIA, rated to withstand bullet impacts up to 44 Remington Magnum caliber. The Kevlar collection box consisted of a cardboard box containing expired Kevlar body armor (mostly NIJ IIIA). The polycarbonate was mounted vertically and the collection box placed at the end of the polycarbonate. Firearms were discharged into the polycarbonate at a shallow angle resulting in slight/moderate bullet deformation. The deflected bullet was then captured by the Kevlar box and recovered. Bullet fragments were generated by firing into a water tank using ammunition that is known to fragment. These fragments are representative of fragments formed when entering a body, but are not necessarily representative of fragments generated when a bullet strikes a hard object. All test fires were placed into labeled envelopes.

3.3   Portable Scanner Evaluation (Aim 2)

Prior to this award, we developed a portable scanning system based on the same underlying GelSight 3D scanning technology (Fig. 1) as our desktop system. The portable unit is self-contained with camera, lens optics, an array of directional lights, and a camera trigger (Fig. 5). Like the desktop system, the portable unit uses a silicone gel pad to improve imaging resolution. The portable scanner fits into a rugged hard case and connects to a laptop computer. The computer's USB port serves as both a communications channel and a power supply for the scanning unit. Therefore the entire scanning operation can be battery powered. The portable scanning optics are mounted on a vertical support and can be manually adjusted using a rack-and-pinion assembly. We have a special version of our TopMatch software with a more restricted interface and simplified scanner controls. From the scan acquisition screen, the user can either register the scanner to a microscale reference or collect a surface scan. Scans are acquired at a lateral sampling of $3.5\mu m$ per pixel. At this resolution scans are rendered extremely quickly ($\sim$5 seconds). This rapid acquisition workflow is amenable to the described in-field, screening, and triage uses. Although

we added some functionality to the portable system, the bulk of the portable scanner was developed prior to this award. The current award evaluated use of the portable scanner.

3.3.1   Cartridge Case Test Set and Data Collection Plan

A data collection and analysis plan was designed to evaluate the scans acquired by the portable system. Note that due to the covid pandemic we were forced to modify some specifics of our data collection plan. Although some details changed, the general themes were maintained. For example, rather than involve students in a simulated outdoor crime scene, we collected some of our data outside in one of our collaborator's yards. Several individuals and several machines were involved in data collection. This allowed us to compare portable vs desktop systems, individual to individual on the same system, and individual to individual on different systems.

Four individuals participated in data collection. Three individuals used the portable system: Todd Weller, Zak Carr, and Madison MacBain. One individual used the desktop system: Ryan Lilien. Todd and Zak are qualified firearms examiners while Madison is a masters student in forensic science and Ryan is a researcher and the principal investigator on this project. During the pandemic, Madison used a portable scanner to collect several thousand scans for inclusion into our core reference dataset. Ryan has collected thousands of scans on the desktop. Therefore, both Madison and Ryan are experts in the use of the portable and desktop systems respectively. Zak and Todd are newer to using the portable system. They received training via an instruction manual and a training overview video produced by Madison. Zak and Todd were asked to collect a number of practice scans on other (different) cartridge cases. These practice scans were digitally transferred to Madison and Ryan who reviewed them for quality. When moving to 3D the most common phenomenon observed is dust in the field of view. Even small pieces of dust are highly visible in a high resolution 3D measurement. It is therefore imperative to thoroughly clean specimens prior to scanning.

Three cartridge cases from each of twelve firearms indicated in Table 1 and Section 3.2 were scanned by all individuals. The same 36 physical cartridge cases were sent from one individual to the next. Cartridge cases were kept in individual envelopes that were marked with the source firearm information. Thumbnail images of one cartridge case from each firearm are shown in Figures 9 and 10. Cartridge cases represent firearms with different breech face class and common calibers (9mm, .40 S&W, 45 ACP).

All systems used a sinusoid microscale reference (R_{sm} appx $135\mu m$, R_a appx $6\mu m$) as a quality control check prior to scanning. A traceability protocol was previously developed where each system

first scans the reference specimen ten times on ten different days to establish a baseline. Then, during scan acquisition a quality control check is performed by measuring the sinusoid one additional time and ensuring that the lateral and depth measurements fell within tolerance. Data on this quality control check is not presented in this report.

3.3.2 Scan Resolution

It is important to note the difference between 'lateral sampling interval' and 'resolution' when referring to any 3D scanning system. Lateral sampling refers to the size (and spacing) between each neighboring pixel. Our desktop system has a lateral sampling of $1.8\mu m$ per pixel and the portable scanner has a lateral sampling of $3.5\mu m$ per pixel. The scan resolution refers to the smallest size features that can be resolved or differentiated on a scan surface. The scan resolution is not typically equal to the lateral sampling. In fact, the Nyquist theorem (from the discipline of signal processing) states that the resolution is typically no better than twice the lateral sampling. That is, with a lateral sampling of $1.8\mu m$ the smallest features one can resolve are typically $3.6\mu m$ apart. However, several factors prevent a system from achieving this 'best' resolution. These factors include the quality of the camera sensor, the quality of the lens, the light used, and the surface reflectivity of the object being imaged. A different camera and lens system is used in our desktop and portable systems. Scans collected off the desktop and portable systems are shown in Figure 6. Note that the desktop scan is slightly more sharp and appears in slightly higher focus. We have design plans to create a higher resolution version of our portable scanner and we have projects underway to increase the resolution of the current hardware. A detailed discussion of resolution is beyond the scope of this report; however, it is possible that the additional detail captured on our desktop system affects the baseline resolution used in each comparison algorithm.

3.3.3 Data Processing

All scans from the portable and desktop scanners were masked by a single individual. Masking a scan involves 'painting' the surface to indicate regions of interest for analysis by the comparison algorithm. That is, algorithms only consider pixels within the designated masked region. For this experiment two regions were masked, the breech-face impression and the aperture shear. Although some of the non-Glock firearms had small transient aperture shears, we did not mask them nor include them in the aperture shear analysis results. Instead, only test fires from the Glocks were used when assessing the aperture shear. All test fires were used when assessing the breech-face impression. We analyzed the scans using

several comparison algorithms as described below. Each algorithm has a base resolution on which it operates. For example, the CMC method starts with resampling scans to $6.25\mu m$/px.

3.3.4 Comparison Algorithms - Cartridge Cases

Four comparison algorithms were used to compare the measured surfaces of the cartridges cases.

- **Breech-Face 1.2** (BF1.2) This comparison algorithm is a feature based method developed by Cadre for comparing two breech-face impressions. It has several internal components for identifying the correct scan alignment and quantifying the similarity among surface features. The score is reported on a scale of 0 (least similar) to 1 (most similar). The BF1.2 function has been tested on several million comparisons and thousands of known matches of scans in our reference collection. We have observed zero false positives (using a threshold of 0.5) and an approximate recall rate of 75-85%. We are now developing this numeric score into a statistical model. Overall, BF1.2 is the highest quality breech-face comparison algorithm we have tested.

- **Aperture Shear 1.2** (AS1.2) This is a Cadre comparison algorithm for quantifying the similarity between two aperture shear striation profiles. The score consists of several internal components for extracting the striation profile, detecting stria, aligning their positions, and quantifying the amount of similarity. Like BF1.2 the score is reported on a scale of 0 (least similar) to 1 (most similar). Overall, AS1.2 is the highest quality aperture-shear comparison algorithm we have tested.

- **Cross Correlation Function** (CCF) The cross correlation function, sometimes referred to by its more full name, the $\mathrm{CCF_{max}}$ is based on a pixel by pixel cross correlation across the entire region of interest. The "max" description refers to the fact that when two surfaces are compared, the cross correlation score is computed for all rotations and translations (*i.e.*, shifts) of one surface relative to the other. The largest cross correlation score (*i.e.*, the max) is reported as the $\mathrm{CCF_{max}}$ or simply CCF score. The CCF can be computed for both breech-face impressions and aperture shears. In the work described here we used the CCF for breech-face impression comparison only. As we will explain below, the CCF score is not a great score for assessing common origin but it is useful when comparing multiple scans of identical test fires.

- **Normalized Convergence Congruent Matching Cells** (Norm-CMC) Over the past decade, NIST has developed a series of comparison algorithms to replace the original CCF function for comparing breech-face impressions. The initial CMC method [13, 14, 19] is based on decomposing the

first surface into a grid of cells and then matching each cell into the second surface. Consistency in the arrangement of the matched cells supports the hypothesis of common origin. There are many named variants of the CMC method and even within a named approach there are multiple different implementations that perform slightly different. The most recent and best performing method is the Convergence method introduced in Chen et. al. [5]. As part of a separate grant from NIST we have implemented the Convergence CMC method into our software. The Normalized Convergence CMC simply divides the number of matched CMC cells by the total number of valid cells. This normalization allows score comparison between test fires with different numbers of detected cells. The typical unnormalized CMC match threshold is 6 cells. Comparisons resulting in 7 or more matches cells are typically considered to have strong support for common origin. To convert this threshold into a normalized framework we assumed that a typical small pistol primer has about 36 valid cells. 6/36 is approximately 0.18. Therefore, Norm-CMC scores above 0.18 can be considered to be above threshold and likely to have common origin. CMC often performs well on well marked surfaces but when run against our real-world core reference collection, CMC does not have as high a recall rate as BF1.2.

Three types of comparisons were made. **Exact** matches involve comparing scans of the same identical specimen made by a different examiner or scanner. For example, the scan of test fire 1 of firearm 3 acquired by examiner 1 compared to the scan of test fire 1 of firearm 3 acquired by examiner 2. **Known Matches (KM)** are pairs of scans that are known to have common origin but which are non-identical specimens. For example, the scan of test fire 1 of firearm 3 compared to the scan of test fire 2 of firearm 3. KMs can be from the same (intra-set) or different (inter-set) operators and equipment. **Known Non-Matches (KNM)** are pairs of scans that are known to have different origin. For example, any test fire from firearm 1 compared to any test fire from firearm 3. KNMs can be from the same or different operators and equipment.

Note that each algorithm has specific uses. The CCF is best at assessing overall similarity among all measured pixels. Therefore the CCF is well-suited for comparing separate measurements of identical specimens but it is not a great way of assessing similarity between known matches (*i.e.*, different test fires from the same firearm). The reason is that every pixel in the masked area contributes to the CCF score. This means that both informative and non-informative pixels have the same ability to affect the score. All masked pixels are in theory informative when comparing identical specimens; however, many surface pixels are not informative when comparing different specimens from the same source. For these

known matches, inconsistent toolmark transfer and regions of surface damage cause some areas of the surface to be more informative than others. Therefore we used the CCF to quantify the similarity among identical specimens.

More sophisticated comparison algorithms, such as our BF1.2, AS1.2, and the NIST CMC methods, attempt to quantify the overall likelihood of common origin. They seek to identify and quantify areas of similar toolmarks. The quality and quantity of these similarities is used to generate an overall similarity score. These methods are more commonly used when searching a database or when computing a statistical level of support for common origin. Therefore, these methods (BF1.2, AS1.2, and CMC), were used when assessing likelihood of common origin between different scan operators or different scanning hardware.

In the Results section we use these score functions to evaluate the scan quality among different individuals and different scanning hardware.

4   Data Results and Analysis

In this section we summarize the experimental results. Results are presented for each aim. Aim 1, Bullet Scanning and Aim 2, Portable Scanner Study. Test fires used in both Aims were collected by our collaborator Zachary Carr as described in Section 3.2.

4.1   Bullet Scanning and Analysis (Aim 1)

4.1.1   Bullet Scanning

Three pristine test fires from each of the ten firearms (Table 1) were scanned using the newly designed bullet holder and bullet tray (Fig. 2). The additions to the TopMatch software for bullet scanning were used to control the scanning process. The entire circumference of each bullet was measured using the bullet roll mechanism described above. All bullets were scanned successfully.

In addition to measuring the conventionally rifled test fires described above we also tested the bullet holder, bullet tray, and bullet rolling mechanism with a polygonal bullet fired from a Glock. Polygonaly rifled bullets are often more minimally marked and the marks observed are less well reproduced. Although there were fewer stria measured in our test, the scan acquisition process and bullet rolling mechanism worked as designed and the scans were successfully obtained.

4.1.2   Bullet Visualization

Measured surfaces can be visualized within our standard 3D viewer; however, the natural curvature of the bullet makes it difficult to visualize all LEA stria at the same time (Fig. 7A). To improve visualization we used a high-pass filter to preserve high-frequency terms (*i.e.*, fine detail) while eliminating bullet curvature. The result of the high-pass filter is a 'flattened' surface. When a virtual light is positioned perpendicular to the flattened surface it is easier to simultaneously view all stria (Fig. 7B). The visualization of measured stria can be further improved by exaggerating (scaling) the z-dimension (Fig. 7C) of a flattened LEA. Z-scaling does not change the original measurement, it is a means of scaling the displayed surface so that stria appear taller but remain in the same position. When comparing striation profiles it is the location of each stria that is important; the absolute magnitudes of each stria are not typically considered. Finally, another visualization approach renders the flattened surface with enhanced contrast (Fig. 7D). We plan on allowing users to use all of these approaches to that we can learn which is the most useful.

4.1.3   Bullet Analysis

After acquisition, each LEA was manually masked within the TopMatch software. We masked the most well-marked region closest to the heel of the bullet. One of the LEA pairs of an identified KMs is shown in Figure 8. Strong agreement between the striation profiles can be seen both on the scan surface and the extracted striation profile.

A linear striation profile was extracted from each LEA and the CMPS algorithm was used to compare all pairs of bullets. When comparing two bullets all LEAs of the first bullet are compared to all LEAs of the second bullet. A score is computed for each rotational alignment as the sum of the corresponding LEA scores. The bullet to bullet comparison score is the largest CMPS sum among the possible alignments. The KM and KNM score distributions are shown in Figure 11 with the distribution for all test fire pairs on the left and the best test fire pair per firearm pair shown on the right. Figure 11 (Right) shows the benefit of collecting and comparing multiple test fires for each firearm. In this graph almost all KNMs score between 10 and 20 while most KMs score above 20. A table of the scores by firearm appears in Table 2.

4.1.4   Damaged Bullets

The newly designed bullet holder, bullet tray, and rolling mechanism work well for undamaged bullets. Because crime scene bullets are often damaged, we explored the ability of our setup to acquire scans of damaged bullets. This preliminary work is a first step towards a general solution for the scanning of damaged bullets. For this part of the project we acquired damaged test fires from the Beretta firearm.

The portable scanner was used to scan bullets with ricochet, mushroomed, and fragment damage. The more physically open nature of the portable scanner allowed easier positioning of the LEA for scanning. Figure 12(Left) shows the bullet holder positioned under the scanning head of the portable scanner. In place of the bullet holder a flat plastic mount can be positioned and damaged bullets can be mounted with mounting putty. In our experiments, a few attempts were sometimes required to get the LEA centered in the field of view. The speed of scan acquisition (less the one second for image capture) means that each optimal LEA position does not need to be held long.

Before scanning the damaged bullets in the portable system we demonstrated that the portable scanner is able to measure pristine samples. We scanned a pristine Beretta test fire on the portable using the setup shown in Figure 12(Left). The bullet scored a CMPS score of 37 when compared to a known match from the same firearm. A score of 37 clearly positions the bullet in the KM portion of the CMPS score distributions (Fig. 11). For comparison, the same pair of bullets scored 44 when both were scanned on the desktop scanner. A pair of matched LEAs between the portable and desktop scans is shown in Figure 13A.

We next used the portable scanner to measure LEAs on the mushroomed bullets and the bullet fragments shown in Figure 4(C & D). To scan the mushroomed bullet we used a plastic tool to bend the petals back to expose the LEAs of interest. An LEA from a mushroomed bullet matched against one from a pristine bullet is shown in Figure 13B. Figure 13C compares a portable fragment scan and a pristine desktop scan. Figure 13D shows a portable fragment scan and a portable pristine scan. Although the portable scans appear slightly less sharp than the desktop scans, strong agreement is clearly visible. We also conducted a proof-of-concept experiment using a holder with a flat foam-pad top. Figure 12(Right) shows a bullet fragment on the flat mount. Figure 13E compares a fragment scanned using this setup on the desktop scanner with a pristine desktop LEA. Scanning of the ricochet bullets was relatively straightforward as there was no interfering metal between the area of interest and the imaging optics.

It is important to note that when scanning damaged bullets it may be necessary to account for distortion in the LEA striation profile. That is, parts of the striation profile may be laterally stretched or

compressed relative to the pristine profile. In future work we will explore the most robust way to account for this distortion. Simplistic scaling or dynamic warping approaches may not be ideal as they could result in higher scores for KNM samples.

The requirement for mounting damaged bullets and exposing the desired surface for visualization suggests that the scanning of damaged bullets will be a challenge for any 3D system. Although it is not typically possible to use our automated bullet tray for all damaged specimens we have demonstrated that it is indeed possible to measure striation profiles from damaged bullets. Despite these promising results, it is likely that some significantly damaged bullets will remain non-scannable due to their deformations. These bullets are likely to be deemed unsuitable for 3D visualization in much the same way that examiners currently consider some damaged specimens unsuitable for analysis via traditional light comparison microscopy.

4.1.5 Bullet Scanning Summary

In the completion of this aim we developed a new bullet holder and bullet tray. An adjustment setting allows the holder to safely mount a wide range of bullet sizes spanning what would be seen in casework. We then developed an automated scanning mechanism using a bullet roll to allow our system to acquire all LEAs without manual intervention. We extended our TopMatch software to support scanning with the new bullet holder. We created an easy to use workflow within the software that guides the user through the acquisition process. The bullet holder, automatic bullet roll, and acquisition software was used to successfully acquire scans from the 30 bullets in our test set. We implemented an LEA flattening visualization procedure which allows the examiner to simultaneously visualize all stria in a curved LEA. When coupled with z-scaling and contrast adjustments this view provides an extremely clear display of the surface. We then compared all measured LEAs (over 14,000 comparisons) using the previously developed CMPS method. We demonstrated that the KNM and KM bullet scores showed good separability. As expected, some firearms produced better marked LEAs than others and this is reflected in their scores. We also noted that our scanner was able to capture surface detail of slippage marks and striated marks in the GEAs. In this aim we also completed proof-of-concept scan acquisition for damaged bullets (ricochet, mushroomed, and fragments). We were impressed that we were able to lift LEAs from the fragments shown in Figure 4(D) and to match these profiles to LEAs on a pristine test fire from the same firearm. This result demonstrates the potential of the portable scanner for bullet acquisition. The optics in the portable scanner are slightly lower resolution than the desktop scanner and so we expected

(and observed) that the portable scans would appear slightly less sharp than the desktop. In future we are planning a series of hardware and software updates for the portable scanner to improve its imaging resolution. Overall, we demonstrated that our TopMatch scanning platform is capable of measuring, visualizing, and comparing pristine and damaged bullets.

4.2 Portable Scanner Study (Aim 2)

In Aim 2, we collected and compared scans acquired by multiple individuals on our portable and desktop scanners. The goal was to establish the scan quality of the portable scanner and to determine if these measurements could be matched against both other portable scanner measurements and measurements from the higher resolution desktop system. We were able to compare scans collected by different individuals, scans collected on two different portable machines, scans collected on the portable vs the desktop machines, and scans collected outdoors vs indoors. A core set of test fires was used to answer each question.

4.2.1 Cartridge Case Scanning

All cartridge cases were scanned as described above (Section 3.3.1). The sinusoid microscale reference was used as a quality control check on all measurements. In addition to the indoor scans, Todd Weller collected scans of test fires from three firearms outdoors during the day in the San Francisco Bay Area. The outdoor scenario was designed to simulate the scanning of evidence at a crime scene. The outdoor setup utilized a battery powered laptop and thus required no wall outlets. The setup could therefore be replicated at any remote location. There were no issues encountered in completing indoor and outdoor scan acquisition. When a user completed their scanning they transferred the scans back to Cadre either via dropbox upload or our Cadre Nexus cloud server. Both approaches are digital transfers over the internet. Scans could therefore be made available at the Cadre offices within minutes of their collection.

Within the results table the data collected by a specific operator on a specific piece of hardware is called a 'Set'. The following Sets and abbreviations are used in this report:

- **P1A**: Portable System 1. Person A. Todd Weller.

- **P1B**: Portable System 1. Person B. Zachary Carr.

- **P2**: Portable System 2. Madison MacBain.

- **D**: Desktop System. Ryan Lilien.

4.2.2 Cartridge Case Comparisons

The score distributions for the Exact, KM, and KNM comparisons are shown in Figure 14. Each distribution in this figure includes all Exact, KM, and KNM comparisons from all individuals and scanners. The distributions for the BF1.2, AS1.2, and Norm-CMC demonstrate several important phenomenon. First, all KNMs score at or near zero. This is an important result and indicates that we don't expect false positives when comparing scans from different operators or different hardware (portable vs. desktop). Second, the KMs for the BF1.2 and AS1.2 score are well above the typical match threshold of 0.5 and in most cases score near 1.0. It is unrealistic to expect that all KMs score near one because some of the selected firearms are minimally marked. Although the Norm-CMC match threshold is 0.18, it appears that the Norm-CMC method does not perform as well as the BF1.2 score when comparing these test fires. In the remainder of this section we break down these distributions.

Exact matches correspond to the comparison of scans of the exact same physical specimen. Because all test fires were sent from one participant to the other, all four participants scanned the exact same specimens. All four scoring functions (BF1.2, AS1.2, CCF, and Norm-CMC) were computed for each pair of scans. Table 3 summarizes the Exact matching results. Each row of the table corresponds to the comparison of scans from two sources. For example, the first row "P2:D" describes the results when comparing P2 scans (Madison MacBain on Portable System 2) to D scans (Ryan Lilien on the Desktop System). The number reported is the mean score and standard deviation for all exact matches. Since there were 36 cartridge cases scanned, these scores represent the mean and standard deviation over those 36 cartridge cases. As expected, BF1.2 is near perfect for all pairs of scans with all scans well above the 0.5 score threshold. The AS1.2 scores are only computed for the two Glock firearms. The AS1.2 scores are a bit lower than one might expect; however, most pairs score above the 0.5 score threshold. There appeared to be one or two test fires with less well marked aperture shears. Because there were only six test fires among these two Glocks, having one or two lower scoring scans can greatly affect the score. The Norm-CMC scores, like the BF1.2 score extremely well. As described above, the BF1.2, AS1.2, and Norm-CMC scores are designed to score well if there is sufficient similarity even if there is some local disagreements among some of the pixels. The CCF function however does not. The CCF function is the best means of quantifying the overall similarity of Exact matches. As expected, all pairs have extremely high CCF scores, typically above 0.8. This result demonstrates that the measurements acquired by each operator on each system are highly consistent and that there is not a significant difference in scans collected by different operators or systems. Figure 14 (Top-Left) shows the CCF score distribution for

the Exact matches, the KM pairs, and the KNM pairs. The KM distribution is centered around higher scores than the KNM distribution but there is a significant amount of overlap. This figure supports the general consensus that the CCF is not a great method for identifying KMs vs KNMs; however, it can be used to evaluate the quality of exact matches. There is one subtle trend in the Exact CCF scores where comparisons between the Desktop and Portable scans appear to have slightly lower CCF (appx 0.84) than those between two Portable scans (appx 0.92). We believe this may be due to the desktop's ability to capture fine detail that is missed by the portable system. In other words, two portable system scans are highly similar because they both miss some of the finest detail; however, the desktop system captures some detail that is missing in the portable. The CCF is likely sensitive to this phenomenon. When comparing a desktop to a portable scan, the CCF quantifies the detail in the higher resolution desktop scans that is missing in the portable scan. When comparing two portable scans the CCF quantifies the fact that they agree on all detail that is present in the scans.

Known Match (KM) scores for Inter-Set comparions are summarized in Table 4. Inter-Set comparisons refer to KMs where the two scans come from different Sets (as defined in Section 4.2.1). That is, the two scans were acquired by different people on potentially different equipment. For each pair of scan Sets, the mean and standard deviation of all KM scores are presented. The BF1.2 and Norm-CMC scores were computed for all cartridge cases and the AS1.2 was only computed for the Glocks. The BF1.2 and Norm-CMC scores are amazingly consistent across all comparisons. The BF1.2 score are well above the typical threshold of 0.5 and the Norm-CMC scores are just above the match threshold of 0.18. As with the exact comparisons, the AS1.2 scores show increased variability because of the small number of test fires included. Known Non-Match scores for Inter-Set comparisons are shown in the distributions of Figure 14. For the BF1.2, AS1.2, and Norm-CMC functions it appears KMs can be reliably identified in scans obtained by different operators and on different hardware.

The mean and standard deviation of all KM scores within each Set (Intra-Set) are shown in Table 5. Intra-Set comparisons refer to KMs where both scans were acquired by the same person on the same equipment. For BF1.2 these numbers are very similar to those of the Inter-Set comparisons (Table 4) indicating that high quality comparisons can be performed on scans collected by different operators and with different hardware. For AS1.2 the small number of samples likely plays into any differences but the numbers are still similar. For Norm-CMC there appears to be a larger difference between Inter-Set and Intra-Set scores. One possible explanation could be varying grid placement across different scanning hardware.

Finally, the max KM scores for each firearm within each set (Intra-Set) are shown in Table 6. Our research agrees with the consensus that there is a benefit to collecting and comparing multiple test fires for each firearm. Taken together, these multiple test fires represent more of the source tool than any one test fire alone. In Table 6, for each firearm we looked at the highest score (*i.e.*, the max score) among all three KMs (test fire 1 vs 2, 1 vs 3, or 2 vs 3) and then computed the mean and standard deviation among all twelve firearms. We also looked at the number of firearms that scored above the specified threshold for the specified score. For example, Set P2 had a KM with a BF1.2 score above 0.5 for ten of the twelve firearms. Sets P1B and D both had all twelve firearms score above a BF1.2 of 0.5. This is particularly impressive for some of the more challenging firearms such as the Beretta (BE40), the Ruger (RU45), the SCCY (SC9), and the Springfield Armory (SP40).

4.2.3 Indoor vs Outdoor Comparisons

In addition to all the indoor scanning, Weller collected scans of the test fires from three of the firearms (CO45, GL240, RU9) outdoors. The comparison scores for just this subset of three firearms is presented in Table 7. The BF1.2 and Norm-CMC KM Inter-Set scores are extremely consistent for these scans. In addition, the CCF Exact comparisons (CCF of the identical test fires as collected under different scenarios) are all extremely high. Table 7 is arranged so that Set X can easily be compared to both Weller's indoors and Weller's outdoor scans (*e.g.*, P2:P1A compared to P2:P1A-OUT). This small experiment suggests that there is no detrimental effect to collecting scans outdoors.

4.2.4 Triage

In many cases the first analysis performed after scan acquisition is triage. Triage refers to sorting the specimens into groups (or clusters) by potential source. It may also involve identifying the most well marked specimen within each group. We implemented a triage graph in our VCM software which can be used with scans acquired either off the desktop or portable scanners. In the graph each scan is represented by a small circle and a line connects two scans if the comparison algorithm score for the corresponding scans is above a specified threshold. Figure 15 shows a screenshot of the triage screen in our software. Shown are the 36 scans collected on the desktop scanner from the 12 firearms in our test set and scored with the BF1.2 algorithm. Note that there are 12 connected groups corresponding to the 12 firearms. Note that 8 of the 12 groups have connections (lines) between all three scans while four groups have only two lines. The missing line indicates that the two corresponding scans did not score high enough. This is

additional support (as described above for bullets) that there is an advantage in collecting multiple test fires for each firearm. Note that Fig. 15 shows no false edges (which would correspond to a false positive link). Selecting the option 'Show highest scoring case per cluster' places a star icon within the circle of the specimen from each cluster with the highest average score to the others within the cluster. This highest scoring case is a candidate for the best exemplar for further database search, for examination, or for use in reports or visualizations. Finally, note that you can select an option to add labels to each circle to know which scan corresponds to which circle. Hovering the mouse over a circle will display the scan ID and show a preview image. Right clicking on a line shows the score of the corresponding scan pair and allows you to load the two scans in the 3D viewer. We think the triage graph will be extremely useful for forensic examiners and technicians. We note that many labs will not want to display comparison scores or a triage graph until after the examiner has completed their analysis. This delayed algorithm approach minimizes the potential influence of a high or low score on an examiner's individual conclusions.

4.2.5   Portable Scanner Summary

In summary, the results of the Exact comparisons support the conclusion that the measurements made on different systems and by different operators are highly similar. The results of the KM comparisons support the hypothesis that KMs involving scans collected by two different operators or on two different machines can be identified. Finally, the results on the KNM comparisons show that we do not expect false positives when comparing across operator or machine.

4.3   Continued Deployment Study

As we have during each of our previous awards, we continue to collaborate with crime labs. Through most of the project period we had a machine setup with the Indiana State Police in Indianapolis. The machine has now moved to the St. Louis County Crime Lab in Missouri. At the beginning of each deployment, Ryan Lilien went down and provided a day of hands-on training to all examiners in the lab. Labs gain practical experience with 3D scanning technology and provide useful feedback to our development team. The covid19 pandemic meant that the Indiana State Police had the lab through most of the project period. We were able to move the system to St. Louis when it was safe to do so. Through deployments like these we continue to collect scan data, to elicit excellent feedback from practitioners, and to train examiners and trainees.

5   Scholarly Products Produced

The primary product of the proposed research is the presentation of our results and progress. There is typically a time delay from completion of a project to its presentation and publication. Thus the research work supported in part by NIJ over the past several years were presented in multiple venues during this project period. Unfortunately the May 2020 AFTE meeting in Austin was canceled due to the pandemic. Fortunately, we are scheduled to present four talks at the August 2021 AFTE meeting in Miami. These include two technical session talks: "3D Virtual Comparison Microscopy within the Crime Lab" and "Results of the 3D Virtual Comparison Microscopy Topography Resolution Study (VCMTRS) for Firearm Forensics" and two workshop presentations: "3D Virtual Comparison Microscopy and Correlation Algorithm Hands-On Practicum" as part of a Comparison Algorithm Workshop and "Introduction to Virtual Comparison Microscopy" as part of the Introduction to VCM Workshop. During both workshops participants will have hands-on time with our virtual microscopy software. They will work through a training tutorial and a virtual proficiency test. We are also scheduled to present an update on Virtual Comparison Microscopy at the Northwest Association of Forensic Scientists in September 2021. During the pandemic year we hosted an online Virtual Comparison Microscopy Workshop for approximately 90 participants to share the results of the VCMTR Study. We gave two VCM presentations at the Midwest Firearm Training Seminar covering results of the VCMTR Study and using VCM for Remote Work Arrangements. Lilien also taught a one hour lecture on VCM at the National Firearms Examiner Academy (NFEA) (Gaithersburg, MD). A final peer-reviewed version of our VCM Error Rate Study was published in the Journal of Forensic Sciences [3]. The above publications and presentations continue our pattern of disseminating our research results. Over the past several years, we have presented at more than 32 forensic conferences and run training sessions for close to twenty local, state, and federal crime labs. We plan to submit both the results of Aims 1 (Bullet Scanning) and 2 (Portable Scanning) to upcoming firearms training seminars and will prepare a paper for publication in a peer-reviewed journal.

6   Summary

We successfully completed the proposed aims during the project period. In Aim 1, we developed a new fixture and process for scanning the surfaces of both pristine and damaged bullets. Part of this new process was the development of an automatic rotation mechanism whereby the scanners existing motorized stage and motorized lift platform could be used to rotate a bullet without user intervention.

This bullet roll process allows unattended scanning of the entire bullet action surface. We developed and demonstrated new ways for visualizing bullet LEAs. We used the CMPS algorithm for the quantitative comparison of LEA striation profiles to validate the quality of the bullet scans acquired. Although it is significantly more difficult to scan damaged bullets than pristine bullets, we demonstrated the ability to acquire LEA scans which are capable of being visually and computationally matched. We demonstrated the measurement and matching of LEAs from shredded bullet fragments and mushroomed bullets. While there is more work to be done we are glad to have achieved this goal.

In Aim 2, we validated use of a portable scanning system and showed that portable scans can be reliably compared against other portable and desktop scans. We scanned a common set of test fires among four participants, at four sites, using three pieces of scanning equipment. We examined the consistency in scans acquired and our ability to recognize Known Matches both within and between scans collected by different individuals at different sites using different scanning hardware. The success of Aim 2 also demonstrates that the workflow for scan acquisition is straightforward and that our training process is successful in enabling new operators (*i.e.*, Todd and Zak) to collect high quality scans.

The completed project developed new tools and techniques for the mathematically grounded analysis of forensic evidence. The ability to scan and compare bullets, including highly damaged bullets, and to collect scans at remote sites, including outdoors, expands the methods available to the firearms and toolmark examiner.

Appendix

Implications for Criminal Justice Policy and Practice

The specific questions investigated, developing new and better 3D tools for bullet scanning and validating a portable 3D scanning unit are of significant importance to the Firearm and Toolmark discipline and the Criminal Justice System. The ability to acquire usable 3D measurements from both pristine and highly damaged specimens may improve an examiners ability to link criminal cases involving the same firearm. This may result in improved accuracy of the forensic product, may provide links between cases where previous techniques may have fallen short, and may prevent incorrect accusations against those who are innocent. In addition, the use of quantitative scoring methods, like CMPS, may soon allow an examiner the ability to include a false match rate or likelihood ratio in their reporting or testimony. This quantitative evaluation will help those in criminal justice weigh the strength of evidence. The validation of a lower-cost, fast, and easy to use portable scanner such as the system in this award may have major impact on forensic science and the criminal justice system. Such a system can be deployed to an active crime scene to provide immediate actionable intelligence to first responders and can lay the initial groundwork for subsequent forensic investigation.

Through this project and our previous NIJ grant awards our primary impact has been the continuing development of a novel 3D imaging and analysis system with reduced cost and improved accuracy compared to existing solutions. Our work directly addresses several aims of the NIJ's Applied Research and Development in Forensic Science for Criminal Justice Purposes program. Through direct collaboration, networking, talks, seminars, and publications we have made many forensic labs (local, state, and federal), practitioners, and policy makers within the criminal justice system aware of this work. The completed project increases the quality and efficiency of forensic analysis, develops new instrumentation systems, and provides a novel approach to enhancing the analysis and interpretation of forensic data derived from physical evidence. The ability to utilize 3D Virtual Comparison Microscopy in actual casework provides examiners a number of functional advantages. Evidence supports the hypothesis that high-quality 3D VCM examination requires less time and results in more accurate conclusions than traditional microscopy. Our work developing 3D scanning and visualization tools and then validating this technology through large examiner-based studies ensures the successful adoption of this technology. As 3D VCM becomes more mainstream it will increasingly benefit the criminal justice system and its ability to present firearm identification and toolmark evidence in the courtroom.

Additional impact will be made as more crime labs become aware of the work and as we continue

to disseminate results. At least twenty crime laboratories have had access to our 3D scanning hardware and now over to three hundred practitioners have had access to our VCM software. This would not have been possible prior to receiving recent NIJ awards. For labs that currently have 2D imaging systems, our 3D system provides a significant improvement in imaging and match accuracy. For labs that currently have competing 3D imaging systems, we feel our system offers more flexibility and transparency with respect to how the scanner works as well as validated hardware and software tools on which conclusions can be based.

Figures and Tables
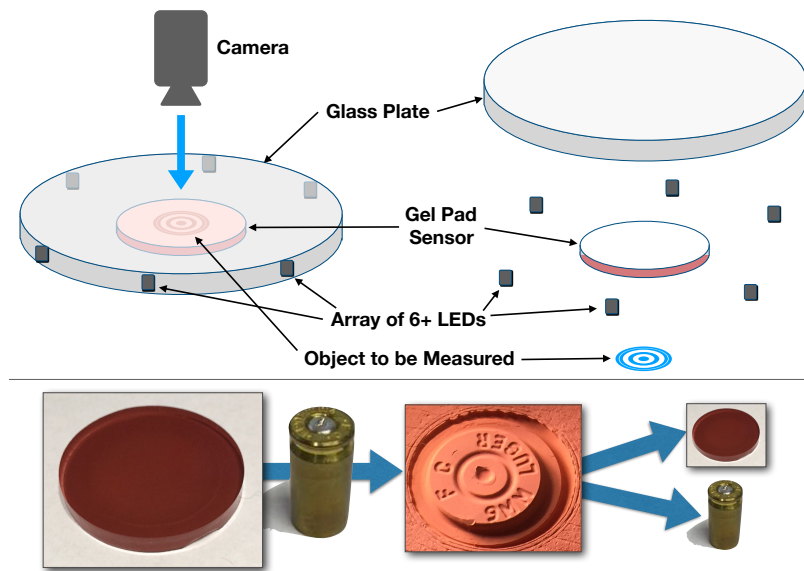
Figure 1: **GelSight Scanning Setup.** Our 3D scanning technique (GelSight) is based on the use of a silicone elastomeric pad with embedded micron-scale thick layer of pigment. (Top Row) The Gel Pad sensor is placed between a glass plate and the item being imaged. When the object to be measured is raised into the gel, the gel and pigment conform to the object (Bottom Row). The gel's pigment removes all unwanted surface reflectance properties (*e.g.*, metal specularity). LED lights are sequentially illuminated and a set of captured images is combined into an accurate 3D surface. In our current scanners, this is an automated process with the camera, lens, glass plate, and LEDs all being fixed and automated. (Bottom Row) A cartridge case is pressed into a gel pad (5mm thick, 38mm diameter) allowing the pigment to conform to the cartridge surface. After scanning the cartridge or bullet is removed and the gel can be used again.
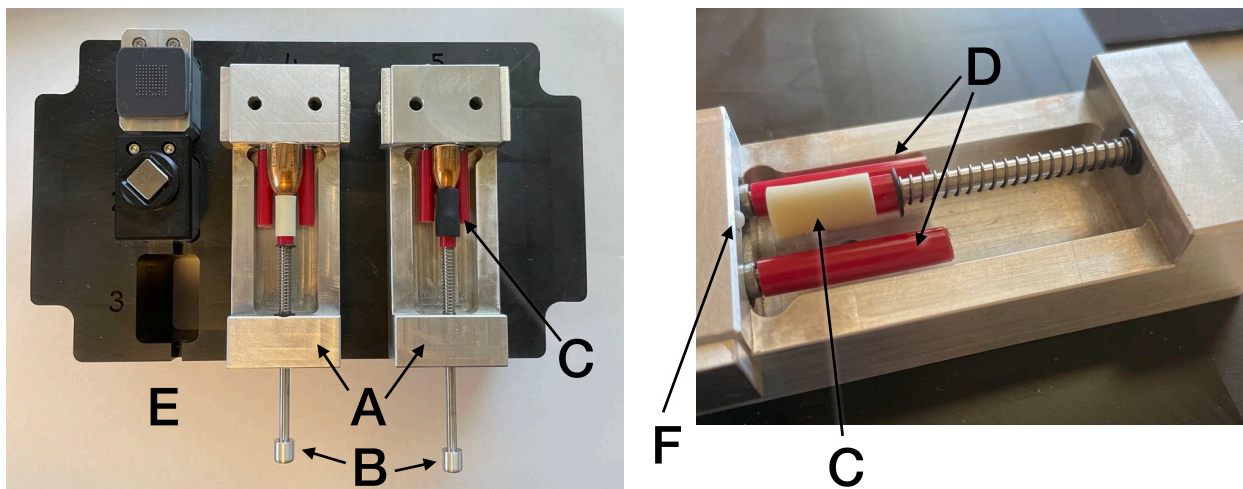

Figure 2: **Bullet Holder in Scan Tray.** (Left) Scanning tray with two bullet holders and a column of smaller holders (E) able to accommodate various microscale references. (Right) Close-up of the bullet holder when it is unloaded. Each bullet holder (A) has a manual rotation knob (B) attached to a spring loaded mount rod. The rod has a rubber cap (C) which is designed to hold the bullet nose and push the bullet base gently against a plastic rear peg (F). The bullet sits on two rubber rollers (D). The spacing between the two rollers can be adjusted by a screw on the bottom of the holder. Adjusting the roller spacing allows the roller to accommodate most bullet diameters.
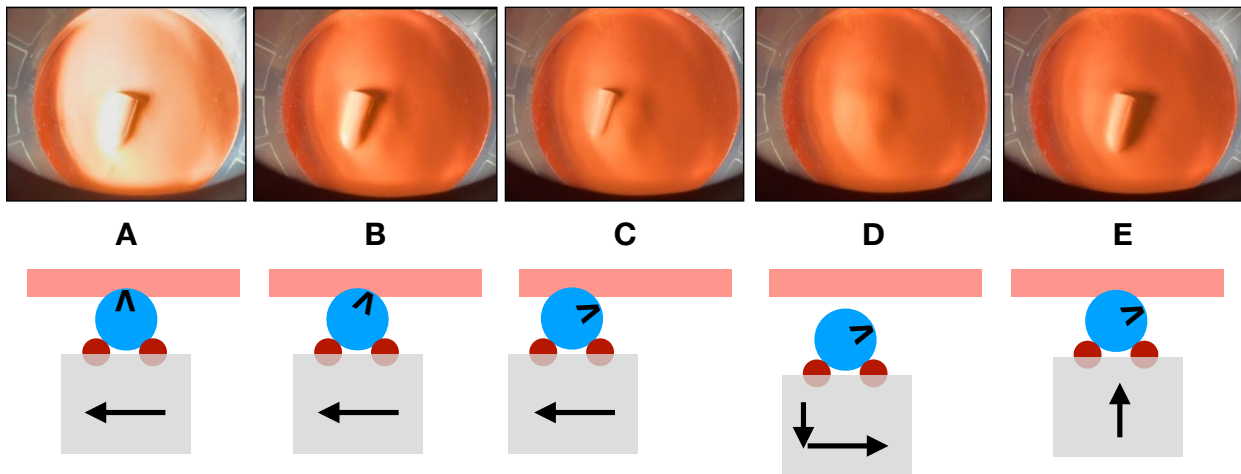
Figure 3: **Bullet Roll Mechanism.** An illustration of the bullet roll mechanism. (Top Row) Photographs of the top of the gel showing the mounted bullet pressed into the gel. (Bottom Row) Schematic figures of the bullet holder cross section with the rubber rollers shown in red and the bullet shown as a blue circle. The following process is implemented and allows an automatic bullet roll. During scanning the bullet is raised into the gel, the system is focused, and a sequence of images is collected allowing measurement of the 3D surface topography. After the images are collected a bullet roll is initiated to move the bullet to the next position. From the starting position (A) the bullet holder is slid slightly to the left (arrow) while the holder is still raised and the bullet is still making contact with the gel. Both the bullet and red rollers spin as the gel grabs the contact surface (B) and (C). After the desired amount of rotation the holder is lowered and shifted back to recenter the now rotated bullet under the gel (D). The rotated bullet is now raised into the gel (E). Large rotations may require more than one cycle through A-E. In all cases we tested only a single rotation is required.
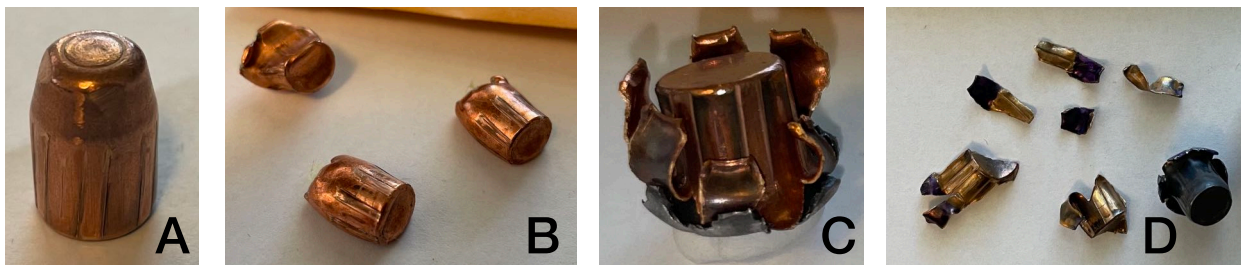

Figure 4: **Bullet Conditions.** Photographs of our test fires showing all four bullet conditions. Pristine (A), Ricochet (B), Mushroomed (C), and Fragmented (D).

Figure 5: **Portable Scanner.** The portable scanner is approximately 12" tall and uses a laptop for scan acquisition and power. A small cartridge case holder consistently positions each cartridge case under the gel pad and imaging optics. When used for bullet scanning the bullet holder (Fig. 2) can be placed under the gel pad an imaging optics.

Number	Firearm	Short Name	Caliber	Rifling	Ammunition	Aims
1	Beretta 96 Brigadier	BE40	.40 S&W	6R	Remington	1,2
2	Colt 1911	CO45	45 Auto	6R	Winchester	1,2
3	Glock 22	GL140	.40 S&W	-	Remington	2
4	Glock 27	GL240	.40 S&W	-	PMC	2
5	Ruger P345	RU45	45 Auto	6R	Winchester	1,2
6	Ruger P95	RU9	9mm Luger	6R	Winchester	1,2
7	SCCY CPX-1	SC9	9mm Luger	7R	Winchester	1,2
8	Smith & Wesson M&P 40	SM40	.40 S&W	5R	Remington	1,2
9	Smith & Wesson SD9VE	SM9	9mm Luger	5R	Winchester	1,2
10	Springfield Armory XD-40	SP40	.40 S&W	6R	Remington	1,2
11	Springfield Armory XDS	SP45	45 Auto	6R	Winchester	1,2
12	Taurus PT111 G2	TA9	9mm Luger	6R	Winchester	1,2

Table 1: **Firearms.** The twelve firearms used in both Aims 1 and 2. The ammunition brand listed is the ammunition used in the pristine bullet test fires and the cartridge cases of Aim 2.
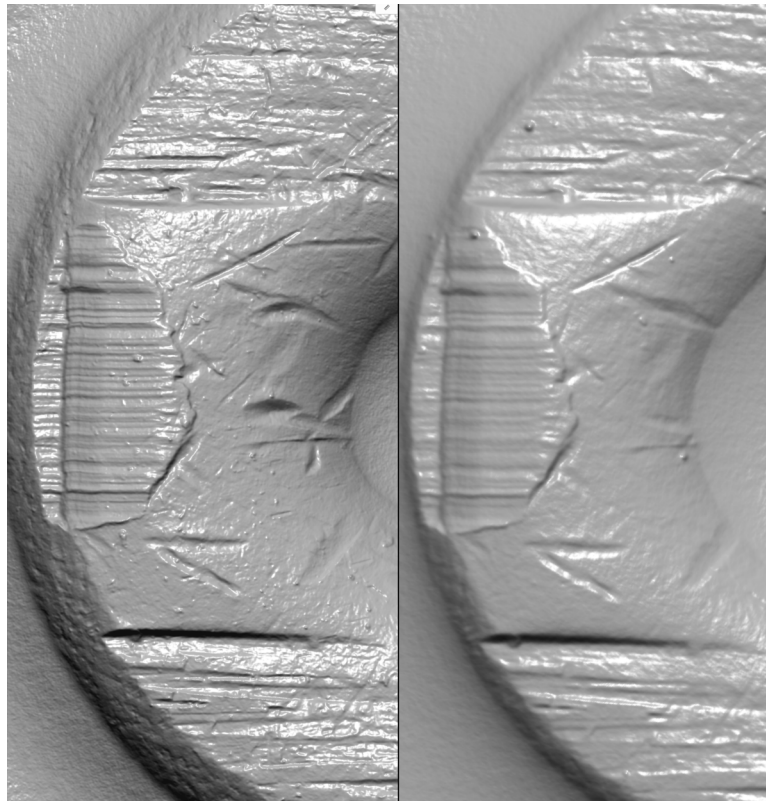
Figure 6: **Desktop and Portable Scan Quality.** Scans of the same Glock test fire are shown as collected on the desktop scanner (left) and the portable scanner (right).

Firearm	CMPS Sum	CMPS Sum / Lands
Beretta 96 Brigadier (BE40)	73	12.1
Colt 1911 (CO45)	25	4.1
Ruger P345 (RU45)	30	5.0
Ruger P95 (RU9)	42	7.0
SCCY CPX-1 (SC9)	44	6.3
Smith & Wesson M&P 40 (SM40)	20	4.0
Smith & Wesson SD9VE (SM9)	34	6.8
Springfield Armory XD-40 (SP40)	24	4.0
Springfield Armory XDS (SP45)	24	4.0
Taurus PT111 G2 (TA9)	29	4.8

Table 2: **Bullet Scores.** CMPS Sum scores for the highest scoring test fire pair for each pair of firearms. The right column is a normalized CMPS score obtained by dividing the CMPS Sum by the number of lands on the bullet. Note that most KNMs have a CMPS Sum less than 20 and a normalized CMPS Sum below 3.5.

Sets	BF 1.2	AS 1.2	CCF	Norm-CMC
P2:D	0.97 (0.04)	0.94 (0.08)	0.81 (0.05)	0.95 (0.06)
P2:P1A	0.97 (0.05)	0.98 (0.03)	0.93 (0.03)	0.94 (0.07)
P2:P1B	0.99 (0.01)	0.80 (0.33)	0.92 (0.03)	0.93 (0.09)
D:P1A	0.97 (0.05)	0.86 (0.16)	0.85 (0.04)	0.94 (0.06)
D:P1B	0.98 (0.04)	0.51 (0.47)	0.84 (0.04)	0.95 (0.06)
P1A:P1B	0.97 (0.05)	0.71 (0.41)	0.93 (0.03)	0.95 (0.07)
Overall	0.98 (0.04)	0.80 (0.31)	0.88 (0.06)	0.95 (0.08)

Table 3: **Exact Scores.** The mean and standard deviation (in parentheses) for Exact match comparisons between the specified scan Sets.
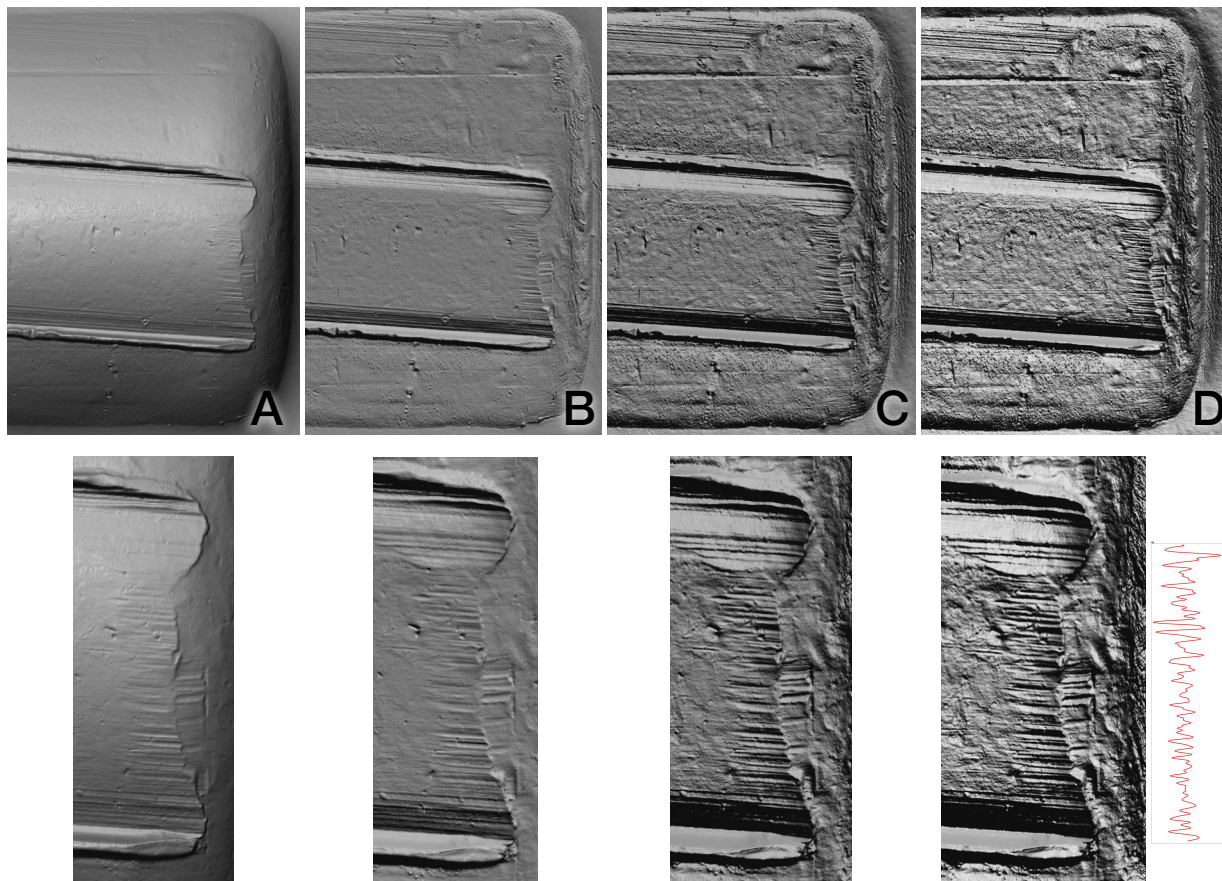
Figure 7: **LEA Flattening.** Flattening the LEA can improve the ability to visualize all stria at the same time. The original LEA is shown in (A). The natural curve of the bullet makes it difficult to position the virtual light for simultaneous visualization of all stria. Panel (B) shows the initial result of flattening. Note the improved ability to simultaneously visualize all stria. Panel (C) shows an exaggerated z-scale of the flattened surface. Panel (D) shows an enhanced contrast view of the flattened surface. Close-ups of each view are shown in the second row. The extracted striation profile is shown in the bottom right.

Sets	BF 1.2	AS 1.2	Norm-CMC
P2:D	0.63 (0.19)	0.89 (0.14)	0.18 (0.16)
P2:P1A	0.63 (0.19)	0.87 (0.13)	0.18 (0.19)
P2:P1B	0.67 (0.20)	0.66 (0.37)	0.19 (0.14)
D:P1A	0.71 (0.21)	0.74 (0.19)	0.22 (0.18)
D:P1B	0.70 (0.21)	0.55 (0.47)	0.24 (0.17)
P1A:P1B	0.68 (0.21)	0.70 (0.31)	0.19 (0.15)
Overall	0.68 (0.23)	0.75 (0.31)	0.21 (0.20)

Table 4: **KM Scores (Inter-Set).** The mean and standard deviation (in parentheses) for Inter-Set KM comparisons. Inter-Set comparisons refer to KMs where the two scans come from different Sets (as defined in Section 4.2.1). That is, the two scans were acquired by different people on potentially different equipment.
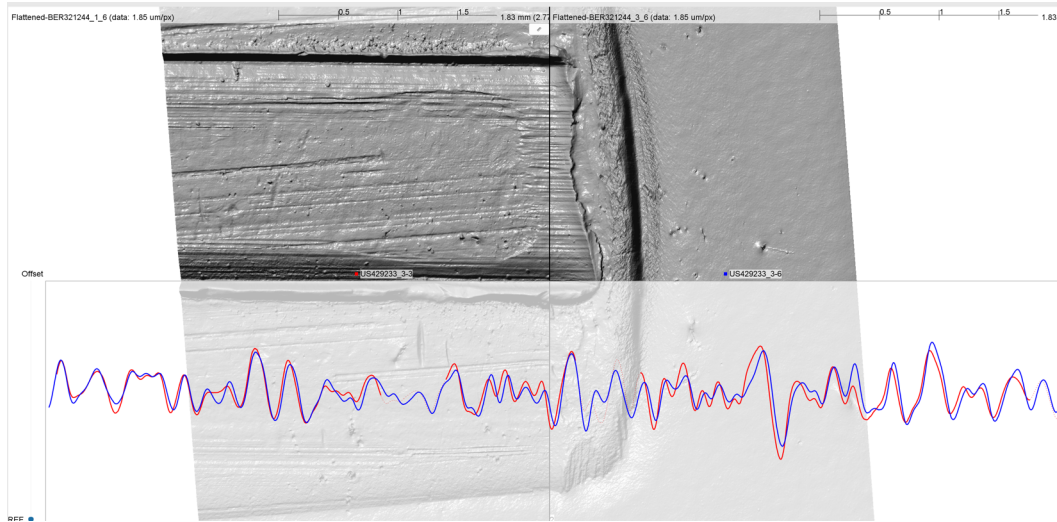
Figure 8: **Matched LEA.** (Top) Flattened view of matched LEAs from two Beretta test fires. (Bottom) Extracted and aligned striation profiles from each LEA. The blue profile is from the right LEA and the red profile is from the left LEA. The blue profile appears as a solid line. The red profile appears solid where it matches the blue profile and dashed where the CMPS algorithm did not identify significant agreement.

Set	BF 1.2	AS 1.2	Norm-CMC
P2	0.63 (0.38)	0.96 (0.05)	0.14 (0.25)
P1A	0.63 (0.39)	0.75 (0.35)	0.31 (0.32)
P1B	0.74 (0.32)	0.47 (0.39)	0.19 (0.25)
D	0.88 (0.25)	0.94 (0.10)	0.31 (0.30)

Table 5: **KM Scores (Intra-Set).** The mean and standard deviation (in parentheses) for Intra-Set KM comparisons. Intra-Set comparisons refer to KMs where both scans were acquired by the same person on the same equipment.

Set	BF 1.2	BF 1.2 > 0.5	AS 1.2	Norm-CMC	Norm-CMC > 0.18
P2	0.83 (0.29)	10 (83%)	0.98 (0.03)	0.30 (0.32)	6 (50%)
P1A	0.84 (0.36)	11 (92%)	0.91 (0.13)	0.51 (0.32)	10 (83%)
P1B	0.95 (0.30)	12 (100%)	0.89 (0.16)	0.30 (0.24)	7 (58%)
D	0.99 (0.22)	12 (100%)	0.99 (0.00)	0.54 (0.30)	11 (92%)

Table 6: **KM Scores (Intra-Set).** The mean and standard deviation (in parentheses) for Intra-Set KM comparisons considering only the highest scoring test fire pair for each KM. Column 'BF1.2>0.5' shows the number of firearms for which there exists a test fire pair with BF1.2 score above 0.5. Column 'Norm-CMC>0.18' shows the number (and percentage) of firearms for which there exists a test fire pair with Norm-CMC score above 0.18. These thresholds are the commonly accepted match thresholds for the respective methods.
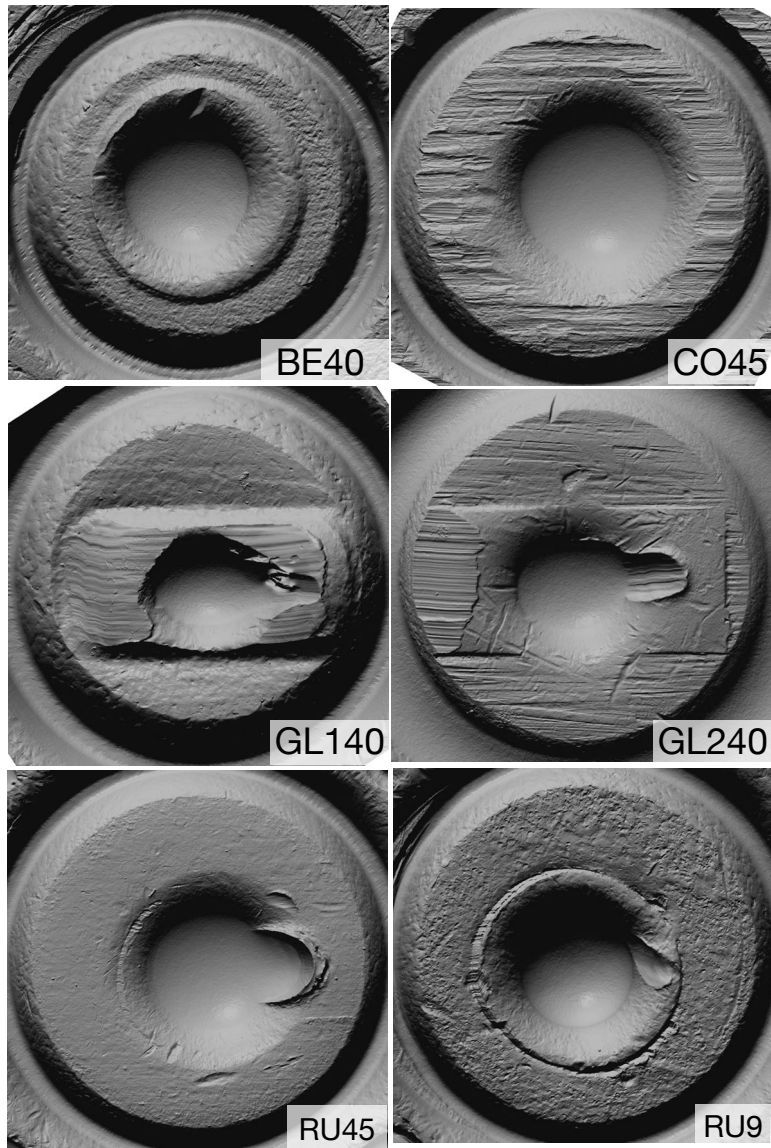
Figure 9: **Test Set Cartridge Cases (Part 1).** Scans of one test fire from the first six firearms in the test set (Table 1) labeled by the firearm's short name.
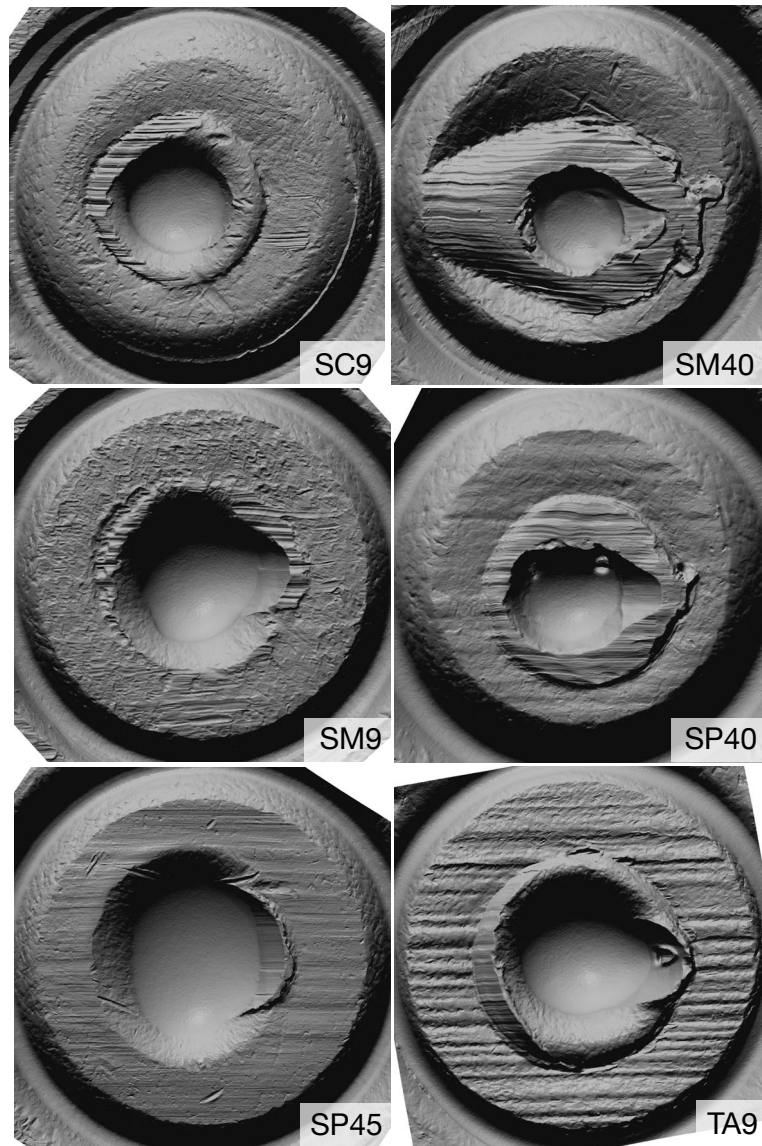
Figure 10: **Test Set Cartridge Cases (Part 2).** Scans of one test fire from the second six firearms in the test set (Table 1) labeled by the firearm's short name.
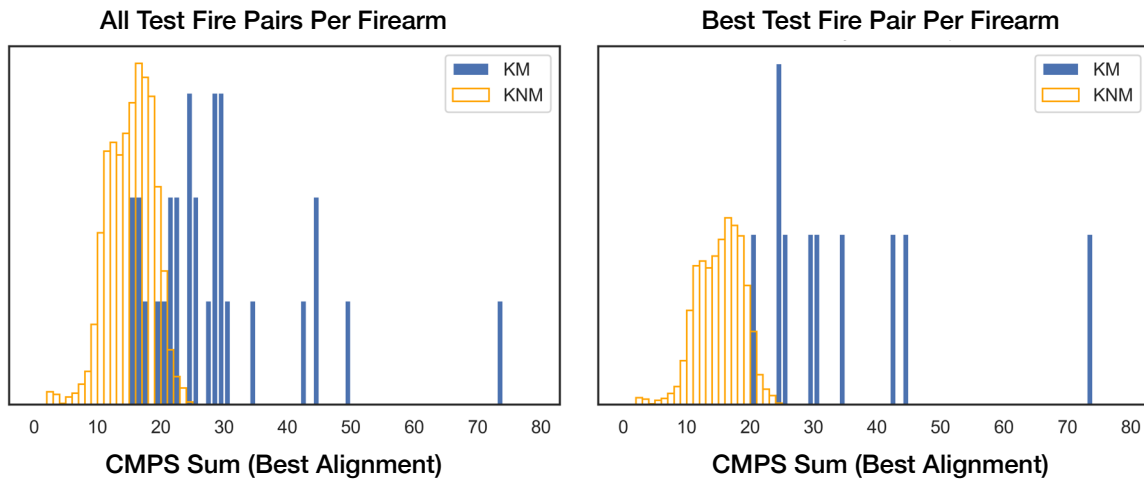
Figure 11: **Bullet Score Distributions.** (Left) CMPS Sum scores at the best alignment for all test fire pairs. (Right) CMPS Sum scores at the best alignment for the highest scoring test fire pair for each pair of firearms.

Figure 12: **Scanning Damaged Bullets.** (Left) The bullet holder positioned in the portable scanner under the scanning head (black). Damaged bullets can be mounted on a plastic base (not shown) and placed under the scanning head in place of the bullet holder shown. (Right) In the desktop scanner a bullet fragment can be positioned mounted on a flat holder in the desktop scanner's scan tray.
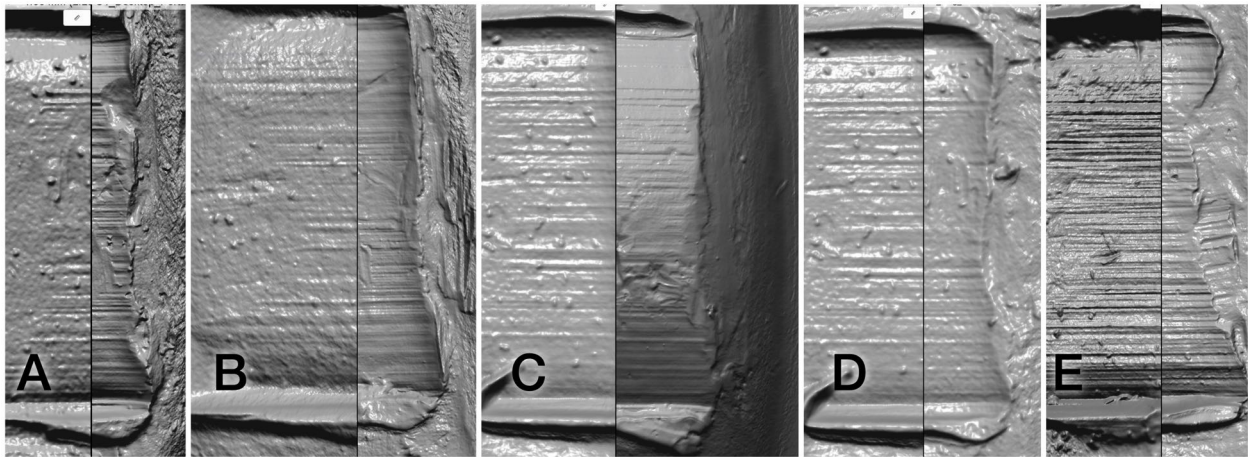
Figure 13: **Damaged Bullet Scanning.** All comparisons shown are KMs (non-exact) from the Beretta (BE40) firearm. (A) Left: Portable Pristine. Right: Desktop Pristine. (B) Left: Portable Mushroomed. Right: Desktop Pristine. (C) Left: Portable Fragment. Right: Desktop Pristine. (D) Left: Portable Fragment. Right: Portable Pristine. (E) Left: Desktop Fragment. Right: Desktop Pristine. Most LEAs are shown flattened.
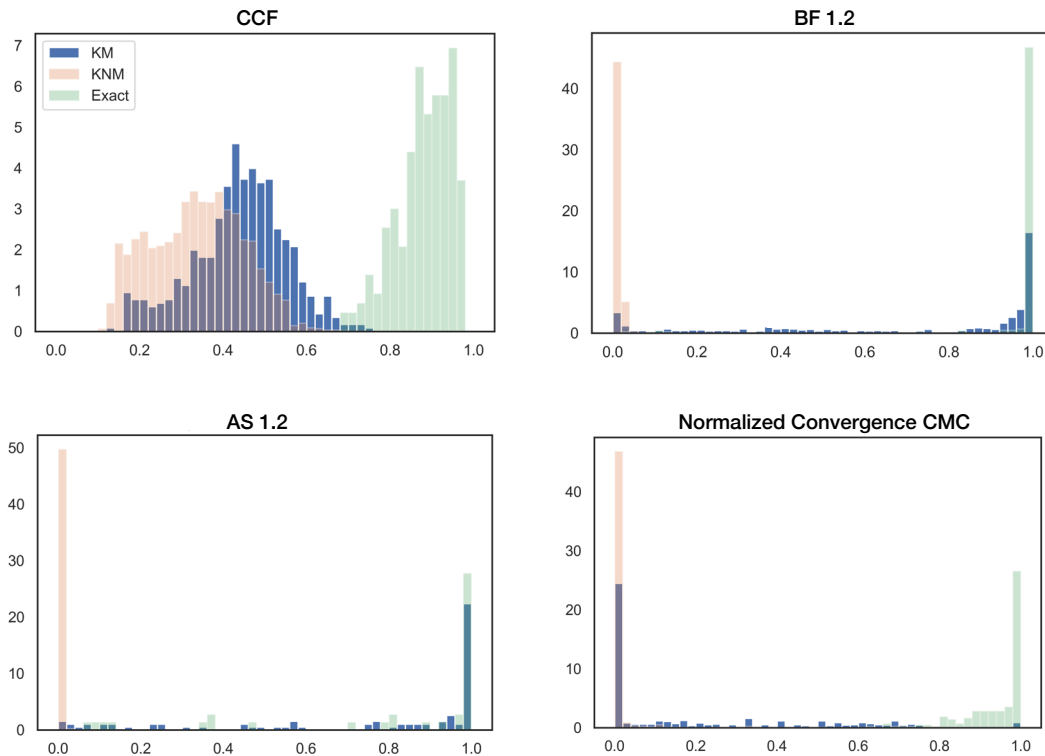

Figure 14: **Cartridge Case Scores.** Score distributions for Known Matches (KM), Exact Matches, and Known-Non Matches (KNM). Shown are distributions for the CCF, Cadre's Breech-Face Impression (BF 1.2), Cadre's Aperture Shear (AS 1.2), and the normalized Convergence CMC.

Sets	KM BF 1.2	KM Norm-CMC	Exact CCF
P2:D	0.77 (0.07)	0.32 (0.20)	0.80 (0.05)
P2:P1A	0.84 (0.08)	0.35 (0.18)	0.94 (0.02)
P2:P1A-OUT	0.83 (0.06)	0.30 (0.16)	0.90 (0.04)
P2:P1B	0.85 (0.07)	0.32 (0.16)	0.91 (0.04)
D:P1A	0.91 (0.07)	0.38 (0.13)	0.85 (0.05)
D:P1A-OUT	0.92 (0.04)	0.45 (0.21)	0.85 (0.05)
D:P1B	0.87 (0.08)	0.44 (0.21)	0.85 (0.03)
P1A:P1A-OUT	0.94 (0.03)	0.53 (0.22)	0.90 (0.04)
P1A:P1B	0.92 (0.04)	0.38 (0.20)	0.93 (0.04)
P1A-OUT:P1B	0.92 (0.04)	0.47 (0.23)	0.90 (0.04)
Overall	0.88 (0.08)	0.40 (0.22)	0.88 (0.06)

Table 7: **Comparison Scores Including the Outdoor Scans.** Columns 'KM BF1.2' and 'KM Norm-CMC' are the mean and standard deviation of the KM Inter-Set scores. Column 'Exact CCF' are the mean and standard deviation of scores between identical specimens. Only the three firearms measured both indoors and outdoors (CO45, GL240, RU9) are included in this table. P1A-OUT is the set measured outdoors.
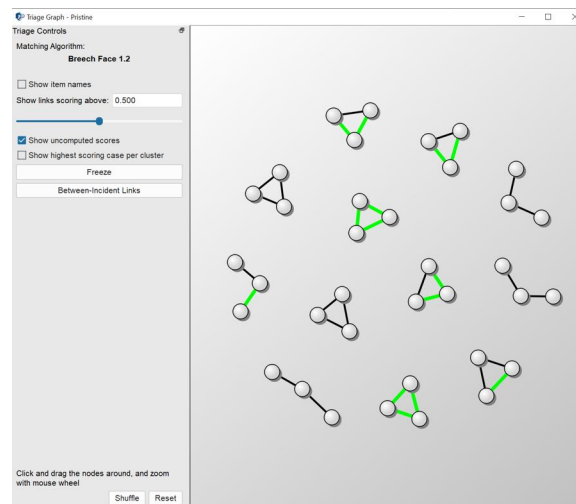

Figure 15: **Triage Graph.** A triage graph can be computed for the scans in one or a pair of incidents. Each scan is represented as a circle. An edge is drawn between two scans if their similarity score is above a threshold (here 0.5). Shown are the twelve firearms of our core cartridge case test set as scanned on the desktop scanner. Twelve clusters can be seen indicating the likely presence of twelve firearms.

References

[1] A. Banno, T. Masuda, and K. Ikeuchi. Three dimensional visualization and comparison of impressions on fired bullets. *Forensic Science International*, 140:233–40, 2004.

[2] R. Bolton-King, P. Evans, C. Smith, J. Painter, D. Allsop, and W. Cranton. What are the prospects of 3D profiling systems applied to firearms and toolmark identification. *AFTE Journal*, 42:23–33, 2010.

[3] C. Chapnick, T. Weller, P. Duez, E. Meschke, J. Marshall, and R. Lilien. Results of 3d virtual comparison microscopy error rate (VCMER) study for firearm forensics. *J. Forensic Sciences*, 66:557–70, 2021.

[4] Z. Chen, W. Chu, J. Soons, R. Thompson, and J. Song. Fired bullet signature correlation using the congruent matching profile segments (CMPS) method. *Forensic Science International*, 305:10–19, 2019.

[5] Z. Chen, J. Song, W. Chu, J. Soons, and X. Zhao. A convergence algorithm for correlation of breech face images based on the congruent matching cells (CMC) method. *Forensic Science International*, 280:213–23, 2017.

[6] W. Chu, M. Tong, and J. Song. Validation tests for the Congruent Matching Cells (CMC) method using cartridge cases fired with consecutively manufactured pistol slides. *AFTE Journal*, 45:361–6, 2013.

[7] M. Johnson and E. Adelson. Retrographic sensing for the measurement of surface texture and shape. *Proc. of the IEEE Conf. on Computer Vision and Pattern Recognition (CVPR)*, pages 1070–7, 2009.

[8] M. Johnson, F. Cole, A. Raj, and H. Adelson. Microgeometry capture using an elastomeric sensor. *ACM Trans. on Graphics, Proc. of SIGGRAPH*, 30:139–44, 2011.

[9] J. Monkres, C. Luckie, N. Petraco, and A. Milam. Comparison and statistical analysis of land impressions from consecutively rifled barrels. *AFTE Journal*, 45:3–20, 2013.

[10] N. Petraco, L. Kuo, H. Chan, E. Phelps, C. Gambino, P. McLaughlin, F. Kammerman, P. Diaczuk, P. Shenkin, N. Petraco, and J. Hamby. Estimates of striation pattern identification error rates by algorithmic methods. *AFTE Journal*, 45:235–44, 2013.

[11] J. Roth, A. Carriveau, X. Liu, and A. Jain. Learning-based ballistic breech face impression image matching. *Proc. of the IEEE Conference on Biometrics (BTAS)*, 2015.

[12] N. Senin, R. Groppetti, L. Garofano, P. Fratini, and M. Pierni. Three-dimensional surface topography acquisition and analysis for firearm identification. *J. Forensic Sciences*, 51:282–95, 2006.

[13] J. Song. Proposed "NIST ballistics identification system (NBIS)" based on 3d topography measurements on correlation cells. *AFTE Journal*, 45:184–94, 2013.

[14] J. Song. Proposed "congruent matching cells (CMC)" method for ballistic identification and error rate estimation. *AFTE Journal*, 47:177–85, 2015.

[15] J. Song, W. Chu, and D. Ott. Proposed congruent matching profile segments (cmps) method for bullet signature correlations. Presented at the Annual Meeting of the Association of Firearm and Toolmark Examiners (AFTE), New Orleans, LA, 2016.

[16] J. Song, T. Vorburger, W. Chu, J. Yen, J. Soons, D. Ott, and N. Zhang. Estimating error rates for firearm evidence identifications in forensic science. *Forensic Science International*, 284:15–32, 2018.

[17] R. Spotts, L. Chumbley, L. Ekstrand, S. Zhang, and J. Kreiser. Optimization of a statistical algorithm for objective comparison of toolmarks. *J. Forensic Sciences*, 60:303–14, 2015.

[18] M. Stocker, R. Thompson, J. Soons, T. Renegar, and A. Zheng. Addressing challenges in quality assurance of 3d topography measurements for firearm and toolmark identification. *AFTE Journal*, 50:104–11, 2018.

[19] M. Tong, J. Song, and W. Chu. An improved algorithm of congruent matching cells (CMC) method for firearm evidence identifications. *J. Research of the National Institute of Standards and Technology*, 120:102–12, 2015.

[20] T. Vorburger, J. Song, and N. Petraco. Topography measurements and applications in ballistics and tool mark identifications. *Surface Topography: Metrology and Properties*, 4:1–35, 2015.

[21] T. Weller, M. Brubaker, P. Duez, and R. Lilien. Introduction and initial evaluation of a novel three-dimensional imaging and analysis system for firearm forensics. *AFTE Journal*, 47:198–208, 2015.

[22] A. Zheng, J. Soons, R. Thompson, J. Villanova, and T. Kakal. 2D and 3D topography comparisons of toolmarks produced from consecutively manufactured chisels and punches. *AFTE Journal*, 46:143–7, 2014.